Closed-form equation for subsidence due to fluid production from a cylindrical confined aquifer

Ayodeji Jayeoba[a], Simon A. Mathias[a,*], Stefan Nielsen[a], Victor Vilarrasa[b], Tore I. Bjørnarå[c]

[a]*Department of Earth Sciences, Durham University, Durham, UK*
[b]*Institute of Environmental Assessment & Water Research, GHS, IDAEA, CSIC, 08028 Barcelona, Spain*
[c]*Norges Geotekniske Institutt (NGI), Oslo, Norway*

Abstract

Ground surface subsidence due to groundwater production is a significant problem. Many attempts have been made to develop analytical models to forecast subsidence rates as a consequence of groundwater production. Previous analytical solutions either make limiting assumptions about the stress regime (e.g., radially symmetric with uniaxial strain or radially symmetric with zero incremental vertical total stress) or assume that the pressure distribution within the aquifer is uniform. Imposing assumptions about the stress regime lead to an overestimate of subsidence. Imposing a uniform pressure assumption often leads to an underestimate of subsidence. In this article, the principle of superposition is applied to extend a previous analytical solution, for a cylindrical uniform pressure change, to allow for a non-uniform pressure distribution resulting from constant rate production of a viscous fluid from a cylindrical confined aquifer of finite permeability. Results from the analytical solution are verified by comparison with a set of fully coupled hydro-mechanical finite element simulations. The analytical solution for subsidence directly above the production well (or uplift above an injection well) can be written in closed-form and is straightforward to evaluate. The equation also shows that, for many practical purposes, ground surface subsidence is insensitive to production fluid viscosity and aquifer permeability when the aquifer radius is less

than the aquifer depth below the ground surface.

Keywords: Subsidence, Groundwater production, Confined aquifer, Analytical solution

1. Introduction

Ground surface subsidence due to groundwater production has been a significant problem around the world for many decades (Gambolati and Teatini, 2015). When water is produced from an aquifer, the pressure within the aquifer is reduced, leading to a reduction in effective stress, which results in subsidence at the ground surface. Many attempts have been made to develop analytical models to forecast subsidence rates as a consequence of groundwater production.

Early models assumed radial symmetry around a groundwater production well. These models then either assumed that strain occurred only in the vertical direction (uniaxial strain) (Verruijt, 1969; Bear and Corapcioglu, 1981a) or that incremental vertical total stress is zero (Verruijt, 1969; Bear and Corapcioglu, 1981b). Verruijt (1969) argues that the zero incremental vertical total stress model is analogous to assuming that the aquifer is overlain by a soft clay overburden, which offers negligible resistance to displacement. Both approaches lead to the elegant result that subsidence, at any point on the ground surface, is linearly proportional to the change in pressure in the aquifer immediately below.

However, the uniaxial strain model overestimates subsidence at the ground surface because it neglects the way the surrounding geological media distributes deformation laterally away from the aquifer of concern (Wu et al., 2018). The zero incremental vertical total stress model also

*Corresponding author. Tel.: +44 (0)1913343491, Fax: +44 (0)1913342301, E-mail address: s.a.mathias@durham.ac.uk

overestimates subsidence at the ground surface because it neglects the vertical resistance of the overburden.

Geertsma (1973) developed an alternative analytical solution whereby the three-dimensional stress distribution is resolved without invoking uniaxial strain or zero incremental vertical total stress assumptions. Specifically, Geertsma (1973) considered the stress, strain and displacement around a cylindrical region of uniform pressure change. In particular, Geertsma (1973) derived a closed-form equation to calculate the ground surface subsidence (induced by the pressure change) immediately above the center of this cylindrical region.

Geertsma's closed-from equation can be related to the ground surface subsidence immediately above a production well at the center of a cylindrical confined aquifer. However, the assumption of uniform pressure leads to an underestimate in ground surface subsidence in this context. This is because the drawdown in pressure at the production well is much more significant than at the far-field of the aquifer (Wu et al., 2018).

Selvadurai and Kim (2015) sought to extend the analytical solution of Geertsma (1973) to allow for a non-uniform pressure distribution controlled by fluid production rate, fluid viscosity and aquifer permeability. However, the resulting equation for ground surface subsidence at the production well is significantly more complicated to evaluate, rendering it beyond application for most practical purposes.

More recently, Pujades et al. (2017) developed a numerical model to look at subsidence above a production well in an unconfined aquifer. They found that the zero incremental vertical total stress model was effective at estimating the subsidence far away from the production well. But close to the production well, the zero incremental vertical total stress model significantly overestimates the

subsidence. Pujades et al. (2017) then derived an empirical correction factor based on studying a sensitivity analysis of their numerical model. However, a limitation of their numerical model was that the model domain was restricted to the extent of the aquifer. Therefore their model was unable to properly account for how fluid production induced deformations propagate out into laterally and vertically extensive geological formations surrounding the aquifer region.

In this article, we build on the work of Geertsma (1973) to develop a closed-form equation for ground surface subsidence due to constant rate production of a viscous fluid from a cylindrical aquifer of finite permeability. This is achieved by application of the principle of superposition. Results from the new analytical solution are compared with equivalent results from a set of finite element simulations obtained using COMSOL Multiphysics v5.4.

2. Mathematical model

The mathematical model in this article is developed as follows. An analytical solution for the pressure distribution around a production well within a confined aquifer is presented. The original analytical solution of Geertsma (1973), for ground surface subsidence due to a cylindrical uniform pressure change, is presented. It is then shown how to incorporate non-uniform pressure distributions, resulting from constant rate production of a viscous fluid from a cylindrical aquifer of finite permeability, using the principle of superposition. A closed-form equation is then derived to calculate the ground surface subsidence directly above the production well.

2.1. Pressure distribution in a confined aquifer

Consider constant-rate single-phase fluid production from a vertically oriented and fully completed production well, of infinitesimally small radius, located in the center of a homogenous,

isotropic, cylindrical and confined aquifer (see Fig. 1a). The pressure distribution, P [$\mathrm{ML^{-1}T^{-2}}$], within the aquifer can be found from (Theis, 1935; Dake, 1983; Mijic et al., 2013)

$$P(r,t) = \begin{cases} P_i - \dfrac{Q\mu}{4\pi kH}\mathrm{E}_1\left(\dfrac{S\mu r^2}{4kt}\right), & 0 < t < t_c \\ \\ P_i - \dfrac{Q\mu}{4\pi kH}\left[\ln\left(\dfrac{R^2}{r^2}\right) + \dfrac{r^2}{R^2} - \dfrac{3}{2} + \dfrac{4kt}{S\mu R^2}\right]F(R-r), & t > t_c \end{cases} \tag{1}$$

where t [T] is time, P_i [$\mathrm{ML^{-1}T^{-2}}$] is the uniform initial pressure of the aquifer prior to commencement of fluid production, Q [$\mathrm{L^3T^{-1}}$] is the constant fluid production rate, μ [$\mathrm{ML^{-1}T^{-1}}$] is the dynamic viscosity of the fluid, k [$\mathrm{L^2}$] is the permeability of the aquifer, H [L] is the thickness of the aquifer, r [L] is radial distance from the production well, S [$\mathrm{M^{-1}LT^2}$] is the specific storage coefficient of the aquifer, R [L] is the radial extent of the aquifer, $F(x)$ denotes the Heaviside step function, $\mathrm{E}_1(x) = -\mathrm{Ei}(-x)$ and $\mathrm{Ei}(x)$ is the exponential integral function and t_c [T] is the characteristic time at which the pressure front, caused by the initiation of fluid production, reaches the boundary of the confined aquifer at $r = R$.

Eq. (1) is exact for $t \gg t_c$ and $t \ll t_c$ but also works as an accurate approximation for $t < t_c$ and $t > t_c$. However, Eq. (1) is not valid in the immediate region around t_c. However, this is of little consequence for our subsequent results. The exact solution to this problem is provided by VanEverdingen (1949). However, their solution is provided as a Laplace transform, which requires numerical inversion, and is therefore not suitable for our subsequent analysis.

Note that the above set of equations represents a flow model, which has been uncoupled from the associated geomechanical processes. However, a good approximation for the pressure distribu-

tion, from a fully coupled flow model, can be obtained using a specific storage coefficient derived assuming zero lateral strain (Gambolati et al., 2000). A recent demonstration was provided by (Andersen et al., 2017). Analogous to Eq. (7.90) of Jaeger et al. (2009, p. 189) and Eq. (6a) of Gambolati et al. (2000), such an expression takes the form

$$S = \frac{\phi}{K_f} + \frac{(1-\alpha)(\alpha-\phi)}{K} + \alpha^2 C_m \tag{2}$$

where ϕ [-] is the porosity, K_f [$\mathrm{ML^{-1}T^{-2}}$] is the bulk modulus of the fluid, α [-] is the Biot coefficient, K [$\mathrm{ML^{-1}T^{-2}}$] is the bulk modulus of the rock and C_m [$\mathrm{M^{-1}LT^2}$] is the vertical (oedometric) bulk compressibility as measured in an oedometer with lateral expansion precluded, found from (Fjær et al., 2008, p.394)

$$C_m = \frac{1}{3K}\left(\frac{1+\nu}{1-\nu}\right) \tag{3}$$

where ν [-] is Poisson's ratio.

The drawdown of the piezometric surface within the aquifer, s [L], can be found from

$$s = \frac{P_i - P}{\rho g} \tag{4}$$

The characteristic time, t_c, can be thought of as the time at which $P = P_i$ at $r = R$ for the $t > t_c$ expression given in Eq. (1). It follows that

$$t_c = \frac{S\mu R^2}{8k} \tag{5}$$

2.2. *Ground surface subsidence due to a cylindrical uniform pressure change*

The geological material surrounding the aquifer is assumed to be homogenous, isotropic, impermeable and semi-infinite. Furthermore, the elastic properties of the surrounding material are assumed to be the same as those of the confined aquifer.

When the change in fluid pressure within the aquifer can be assumed uniform, Eq. (1) reduces to

$$P = P_i - \frac{Qt}{\pi H S R^2}, \quad 0 \leq r \leq R \tag{6}$$

and the subsidence at the surface directly above the production well, w [L], can be found from (Geertsma, 1973; Fjær et al., 2008, p. 405)

$$w = 2C_m H\alpha(P_i - P)(1-\nu)\left(1 - \frac{D}{\sqrt{D^2+R^2}}\right) \tag{7}$$

where D [L] is the depth of the center of the aquifer from the ground surface.

Substituting Eq. (6) into Eq. (7) leads to

$$w = \frac{2C_m\alpha(1-\nu)Qt}{\pi S R^2}\left(1 - \frac{D}{\sqrt{D^2+R^2}}\right) \tag{8}$$

Geertsma (1973) also derived analytical solutions for displacement in the radial and vertical directions, $u_r(r,z)$ [L] and $u_z(r,z)$ [L], respectively, normal total stress in the radial, angular and vertical directions, $\sigma_r(r,z)$ [$\mathrm{ML^{-1}T^{-2}}$], $\sigma_\theta(r,z)$ [$\mathrm{ML^{-1}T^{-2}}$] and $\sigma_z(r,z)$ [$\mathrm{ML^{-1}T^{-2}}$], respectively, and the stress, $\tau_{rz}(r,z)$ [$\mathrm{ML^{-1}T^{-2}}$] for this case. Note that z [L] is depth from the ground surface and r [L] is, again, the horizontal distance from the center of the well. In this way it can be

understood that $w = -u_z(0,0)$ (see Fig. 1b). These analytical solutions are substantially more complicated to evaluate as compared to Eq. (7) because they involve numerical approximations of several integral expressions. Nevertheless, all the mathematical expressions needed to determine these analytical solutions are presented in Appendix D5 of Fjær et al. (2008).

Because the problem being solved is a linear elastic problem, all the analytical solutions presented in Appendix D5 are linearly proportional to $P - P_i$. It is therefore useful to define the following auxiliary terms:

$$\tilde{w}(R) = \frac{w}{P - P_i}, \quad \tilde{u}_j(r,z,R) = \frac{u_j(r,z,R)}{P - P_i}, \quad \tilde{\sigma}_j(r,z,R) = \frac{\sigma_j(r,z)}{P - P_i}, \quad \tilde{\tau}_{rz}(r,z,R) = \frac{\tau_{rz}(r,z)}{P - P_i} \tag{9}$$

where j is r for radial direction and z for vertical direction and the w, u_j, σ_j and τ_{rz} terms in Eq. (9) hereafter specifically relate to the expressions presented in Appendix D5 of Fjær et al. (2008). Note that we are also identifying these expressions are functions of the radius of the uniform pressure cylinder, R, which corresponds to the radius of the confined aquifer in this case. For example, from Eq. (7),

$$\tilde{w}(R) = -2C_m H\alpha(1-\nu)\left(1 - \frac{D}{\sqrt{D^2 + R^2}}\right) \tag{10}$$

2.3. Ground surface subsidence due to production of a viscous fluid

The analytical solutions presented by Geertsma (1973) explicitly assumes that the pressure within the aquifer is uniform. However, it is possible to derive approximate solutions to allow for non-uniform pressures by discretising the pressure distribution and applying the principle of superposition as follows:

Let $r \in [0, R]$ be discretized into N, not necessarily equally spaced, points located at r_k where $k = 1, 2, 3, \ldots, N$ (see Fig. 1c). In this way it can be said that:

$$w \approx \sum_{k=2}^{N} \tilde{w}(r_{k-1/2})(P_{k-1} - P_k) \tag{11}$$

$$u_j(r, z) \approx \sum_{k=2}^{N} \tilde{u}_j(r, z, r_{k-1/2})(P_{k-1} - P_k) \tag{12}$$

$$\sigma_j(r, z) \approx \sum_{k=2}^{N} \tilde{\sigma}_j(r, z, r_{k-1/2})(P_{k-1} - P_k) \tag{13}$$

$$\tau_{rz}(r, z) \approx \sum_{k=2}^{N} \tilde{\tau}_{rz}(r, z, r_{k-1/2})(P_{k-1} - P_k) \tag{14}$$

where

$$r_{k-1/2} = \frac{r_k + r_{k-1}}{2} \tag{15}$$

2.4. Closed-form equation for subsidence above the production well

The series expansion of the $\mathrm{E}_1(x)$ function takes the form (Cooper and Jacob, 1946)

$$\mathrm{E}_1\left(\frac{S\mu r^2}{4kt}\right) = -\gamma - \ln\left(\frac{S\mu r^2}{4kt}\right) + O\left(\frac{S\mu r^2}{4kt}\right) \tag{16}$$

where $\gamma = 0.5772$ is known as the Euler-Mascheroni constant.

It follows that Eq. (1) can be written as (considering Cooper and Jacob, 1946)

$$P(r,t) = \begin{cases} P_i - \dfrac{Q\mu}{4\pi kH}\ln\left(\dfrac{r_e^2}{r^2}\right)F(r_e - r) + O\left(\dfrac{S\mu r^2}{4kt}\right), & 0 < t < t_c \\ \\ P_i - \dfrac{Q\mu}{4\pi kH}\left[\ln\left(\dfrac{R^2}{r^2}\right) + \dfrac{r^2}{R^2} - \dfrac{3}{2} + \dfrac{4kt}{S\mu R^2}\right]F(R - r), & t > t_c \end{cases} \tag{17}$$

where r_e [L] can be thought of as the radius of influence of the production well, found from

$$r_e = \sqrt{\frac{4kte^{-\gamma}}{S\mu}} \tag{18}$$

Because of the simple forms of Eqs. (17) and (7), an exact solution for w can be obtained by considering

$$w = \int_0^R \tilde{w}(r)\frac{dP}{dr}dr \tag{19}$$

Differentiating Eq. (17) with respect to r leads to

$$\frac{dP}{dr} = \frac{Q\mu}{2\pi kH}\begin{cases} \dfrac{1}{r}F(r_e - r) + O\left(\dfrac{S\mu r}{4kt}\right), & 0 < t < t_c \\ \\ \left(\dfrac{1}{r} - \dfrac{r}{R^2}\right)F(R - r) + \left(\dfrac{2kt}{S\mu R^2} - \dfrac{1}{4}\right)\delta(R - r), & t > t_c \end{cases} \tag{20}$$

where $\delta(x)$ is the Dirac delta function.

It follows that

$$w_D = \begin{cases} 4\ln\left[\frac{1}{2}\left(1+\sqrt{1+\frac{\epsilon e^{-\gamma} t_D}{2}}\right)\right], & 0 < t_D < 1 \\ \\ \left(1-\frac{1}{\sqrt{1+\epsilon}}\right)(t_{0D}+t_D), & t_D > 1 \end{cases} \tag{21}$$

where

$$t_{0D} = \left(1-\frac{1}{\sqrt{1+\epsilon}}\right)^{-1}\left[4\ln\left(\frac{1+\sqrt{1+\epsilon}}{2}\right)+\frac{4+5\epsilon}{\epsilon\sqrt{1+\epsilon}}-\frac{4}{\epsilon}-3\right] \tag{22}$$

and

$$w_D = \frac{4\pi k w}{Q\mu C_m \alpha(1-\nu)}, \quad t_D = \frac{8kt}{S\mu R^2}, \quad \epsilon = \frac{R^2}{D^2} \tag{23}$$

It can be seen that the deviation of Eq. (21) from the original solution for a uniform pressure distribution, Eq. (8), is controlled by the value of t_D. When $t_D \gg t_{0D}$, Eq. (21) reduces to Eq. (8). High t_D values imply high permeability, long production duration, low compressibility, low viscosity and/or small aquifer radius. From Eq. (22), it can be shown that $t_{0D} < 1$ when $\epsilon < 3.453$. It follows that if $t_D > 1$, ground surface subsidence can be calculated to a reasonable accuracy using a uniform pressure distribution providing the radius of the aquifer is a lot less than 1.858 times the depth of the aquifer below the ground surface. This further implies that, for many practical purposes, ground surface subsidence is insensitive to production fluid viscosity and aquifer permeability when the aquifer radius is less than the aquifer depth.

3. Finite element modeling

Results from the analytical solution were compared with results from four equivalent finite element (FE) simulations, described by the parameter values given in Table 1. These simulations

were obtained using COMSOL Multiphysics v5.4.

Cases 1 and 3 in Table 1 are relatively shallow scenarios with the aquifers situated at a depth of 200 m. In contrast, Cases 2 and 4 are deeper scenarios with the aquifers situated at a depth of 1000 m. Cases 1 and 2 are based on the Berea sandstone properties presented in Table 7.2 of Jaeger et al. (2009). Cases 3 and 4 are based on a softer rock with a Bulk modulus an order of magnitude less than that for the Berea sandstone.

The FE simulations involved full hydro-mechanical coupling such that changes in fluid pressure result in changes in volume of the porous material and deformation whilst concomitant changes in stress results in a change in fluid pressure. Fluid production is specified as an outward mass flux on a vertical well segment along the radial symmetry axis. Since the formation surrounding the aquifer is assumed to be impervious, the aquifer has no-flow boundary conditions on all other boundaries. To simulate an infinitely large domain outside of the aquifer, the lateral and lower sides of the formation surrounding the aquifer is padded with infinite element domains. These domains have a geometrical scaling corresponding to an extent of several hundred kilometers, enough for the stress perturbation (caused by fluid production) not to reach the outer boundary of the computational model. The associated boundaries are treated as zero deformation boundaries. In contrast, the free surface upper boundary is treated as a zero traction boundary.

Pressure dissipation is fast in nearly incompressible fluids and formations. Since the aquifer is confined, there are no particularly large gradients in the solution for the fluid pressure or the displacement that require a particularly fine computational grid. The mesh used therefore consists of a fairly uniform grid with a maximum grid size of 125 meters, mainly to ensure a high resolution in the output for presentation of the results.

The FE models were constructed using COMSOL's core functionality and did not require the use of any additional application packages. The relevant equations used are described in Sections 3 and 4 of Bjørnarå (2018). Spatial discretisation was achieved using default quadratic Lagrange elements. Solution was achieved using COMSOL's direct solver, MUMPS (MUltifrontal Massively Parallel sparse direct Solver).

4. Results

Fig. 2 shows plots of drawdown and ground surface subsidence as a function of radial distance from the production well for different times. The results from the finite element simulations are shown as circular dots. The results from the analytical solution are shown as solid lines. Drawdown was calculated using Eq. (1) and subsidence was calculated using Eq. (12). To perform the superposition, $r \in [R \times 10^{-3}, R]$ was discretised into 100 logarithmically spaced points. Logarithimic spacing is required to properly capture the steep pressure gradients that occur close to the production well. Also shown, as circular markers, are values of subsidence directly above the production well, calculated using the closed-form equation given by Eq. (21).

The results from the fully coupled hydro-mechanical finite element simulations and the analytical solution are very similar, confirming that the uniaxial strain assumption involved in the definition of storativity, S, in Eq. (2) is appropriate in this context, as previously shown by Gambolati et al. (2000). The results from the closed-form equation, given by Eq. (21), correspond increasingly well with Eq. (12) with increasing time. This is to be expected because the associated approximation of the pressure profile, given by Eq. (17), assumes that $t_D \gg 1$. Despite this shortcoming, Eq. (21) provides very close estimates of the subsidence calculated by Eq. (12). The

advantage of Eq. (21) is that it is significantly more straightforward to evaluate, as compared to Eq. (12).

Looking at Fig. 2a it can be seen that the radius of influence moves out from the well until just after 30 days, when it reaches the aquifer boundary, at a radial distance of 3000 m. After this point, pressure across the aquifer increases in a relatively uniform fashion. After 300 days of water production, the drawdown in the aquifer ranges from 8 to 12 m. For the shallow case (i.e., Fig. 2b), the subsidence above the well reaches a maximum value of just over 0.6 mm. This appears relatively uniform throughout the confined aquifer. The subsidence then decreases to zero at 1000 m from the edge of the aquifer. For the deeper case, the maximum subsidence is reduced but subsidence persists much further away from the aquifer boundary (see Fig. 2c).

The softer rock scenarios, Cases 3 and 4, lead to less drawdown in the aquifer (see Fig. 2d). However, this is compensated for by a greater level of subsidence at the ground surface (compare Figs. 2b and e and 2c and f). It is also noted that the radius of influence takes longer to reach the aquifer boundary. This is due to the reduction in t_c caused by the reduction in bulk modulus (recall Eq. (5)). The non-uniform pressure profile in the aquifer is clearly pronounced in the surface subsidence profile for the shallow scenario depicted in Fig. 2e. However, the subsidence profile is much smoother at 1000 m depth (see Fig. 2f).

5. Conclusions

Geertsma (1973) provided an analytical solution, which can be used to calculate the ground surface subsidence due to a cylindrical uniform pressure change. In this article, the principle of superposition was used to build on the work of Geertsma (1973) to develop an analytical solution

for ground surface subsidence due to constant rate production of a viscous fluid from a cylindrical aquifer of finite permeability. Results from the analytical solution were verified by comparison with a set of fully coupled hydro-mechanical finite element simulations.

The analytical solution based on the principle of superposition requires a priori discretisation of the pressure distribution. However, using Geertsma's closed-form equation to describe ground surface subsidence directly above the center of the cylindrical uniform pressure change, it was also possible to derive a simple closed-form equation to describe ground surface subsidence directly above the production well (or uplift directly above an injection well) within the aforementioned aquifer. The resulting equation relates a dimensionless subsidence to a dimensionless time, with just one free dimensionless parameter, which represents the ratio of the aquifer radial extent to the aquifer depth. Furthermore, the equation shows that, for many practical purposes, ground surface subsidence is insensitive to production fluid viscosity and aquifer permeability when the aquifer radius is less than the aquifer depth below the ground surface.

Acknowledgements

We are grateful for funding received from the Nigerian Tertiary Education Trust Fund in conjunction with the University of Ibadan, Ibadan, Nigeria.

References

Andersen, O., Nilsen, H. M., Gasda, S. (2017), Modeling geomechanical impact of fluid storage in poroelastic media using precomputed response functions. Computational Geosciences, 21, 1135–1156.

Bear, J., & Corapcioglu, M. Y. (1981a). Mathematical model for regional land subsidence due to pumping: 1. Integrated aquifer subsidence equations based on vertical displacement only. Water Resources Research, 17, 937–946.

Table 1: Parameter values used to obtain the results presented in Fig. 2.

Parameter	Case 1	Case 2	Case 3	Case 4
Depth of aquifer, D (m)	200	1000	200	1000
Radius of aquifer, R (m)	3000	3000	3000	3000
Aquifer thickness, H (m)	100	100	100	100
Production rate, Q ($m^3 day^{-1}$)	100	100	100	100
Bulk modulus, K (GPa)	8.0	8.0	0.8	0.8
Poisson's ratio, ν (-)	0.2	0.2	0.2	0.2
Biot coefficient, α (-)	0.8	0.8	0.8	0.8
Porosity, ϕ (-)	0.19	0.19	0.19	0.19
Permeability, k (m^2)	190×10^{-15}	190×10^{-15}	190×10^{-15}	190×10^{-15}
Fluid density, ρ (kg m^{-3})	1000	1000	1000	1000
Dynamic viscosity, μ (Pa s)	10^{-3}	10^{-3}	10^{-3}	10^{-3}
Fluid modulus, K_f (GPa)	2.1	2.1	2.1	2.1
Aspect ratio, $\epsilon = R^2/D^2$ (-)	225	9	225	9
Value of t_D at 300 days (-)	29.30	29.30	6.872	6.872

Bear, J., & Corapcioglu, M. Y. (1981b). Mathematical model for regional land subsidence due to pumping: 2. Integrated aquifer subsidence equations for vertical and horizontal displacements. Water Resources Research, 17, 947–958.

Bjørnarå, T. I. (2018). Model development for efficient simulation of CO2 storage. PhD Thesis. University of Bergen.

Cooper, H. H., & Jacob, C. E. (1946). A generalized graphical method for evaluating formation constants and summarizing well-field history. EOS, Transactions American Geophysical Union, 27, 526–534.

Dake, L.P. (1983), Fundamentals of Reservoir Engineering, Elsevier.

Fjær, E., Holt, R. M., Horsrud, P., Raaen, A. M., & Risnes, R. (2008), Petroleum Related Rock Mechanics - 2nd Editon, Elsevier.

Gambolati G, Bau, D., Teatini, P., & Ferronato, M. (2000). Importance of poroelastic coupling in dynamically active aquifers of the Po river basin, Italy. Water Resources Research, 36,2443–2459.

Gambolati, G., & Teatini, P. (2015). Geomechanics of subsurface water withdrawal and injection. Water Resources Research, 51, 3922–3955.

Geertsma, J. (1973), Land subsidence above compacting oil and gas reservoirs. J. Petr. Tech., 25, 734–744.

Jaeger, J. C., Cook, N. G., & Zimmerman, R. (2009). Fundamentals of Rock Mechanics. John Wiley & Sons.

Mijic, A., Mathias, S. A., & LaForce, T. C. (2013), Multiple Well Systems with Non-Darcy Flow. Groundwater, 51, 588–596.

Pujades, E., De Simone, S., Carrera, J., Vazquez-Sune, E., & Jurado, A. (2017). Settlements around pumping wells: Analysis of influential factors and a simple calculation procedure. Journal of Hydrology, 548, 225–236.

Selvadurai, A. P. S., & Kim, J. (2015). Ground subsidence due to uniform fluid extraction over a circular region within an aquifer. Advances in Water Resources, 78, 50–59.

Theis, C. V. (1935). The relation between the lowering of the piezometric surface and the rate and duration of discharge of a well using ground-water storage. EOS, Transactions American Geophysical Union, 16, 519–524.

Van Everdingen, A. F., & Hurst, W. (1949). The application of the Laplace transformation to flow problems in reservoirs. Journal of Petroleum Technology, 1(12), 305–324.

Verruijt, A. (1969). Elastic storage of aquifers. In Flow Through Porous Media, Edited by R. J. M. DeWiest, 331-376, Academic, New York.

Wu, G., Jia, S., Wu, B., & Yang, D. (2018). A discussion on analytical and numerical modelling of the land subsidence induced by coal seam gas extraction. Environmental Earth Sciences, 77, 353.

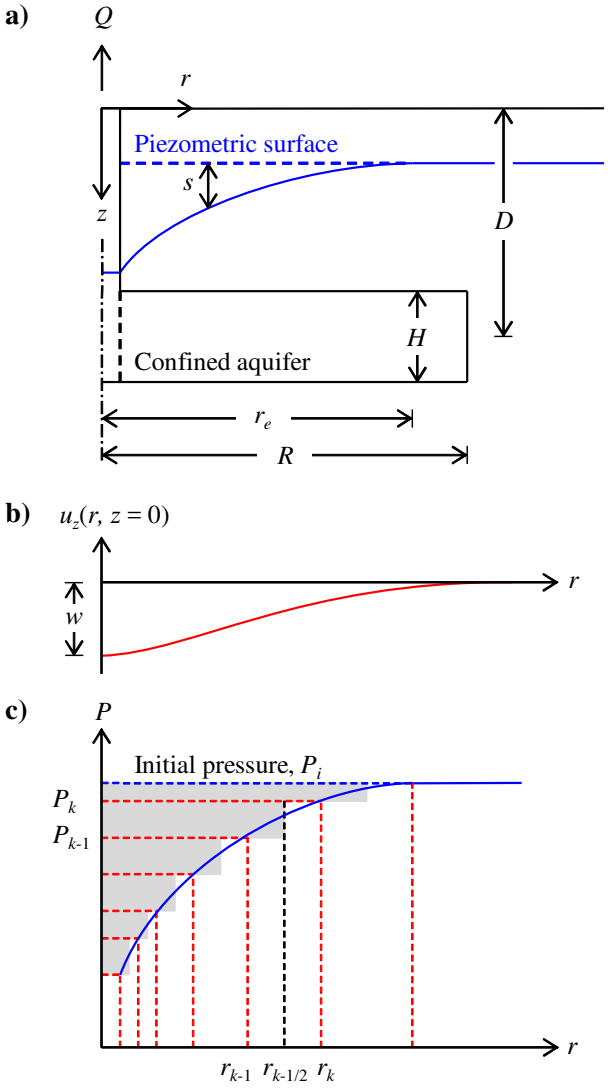

Figure 1: Schematic diagrams showing: a) The production well and its relation to the confined aquifer and surrounding semi-infinite geological formation. b) The maximum subsidence above the production well and the vertical displacement, $u_z(r, z)$, at the ground surface (i.e., $z = 0$). c) How the pressure is discretised to apply the principle of superposition for Eqs. (11) to (14).

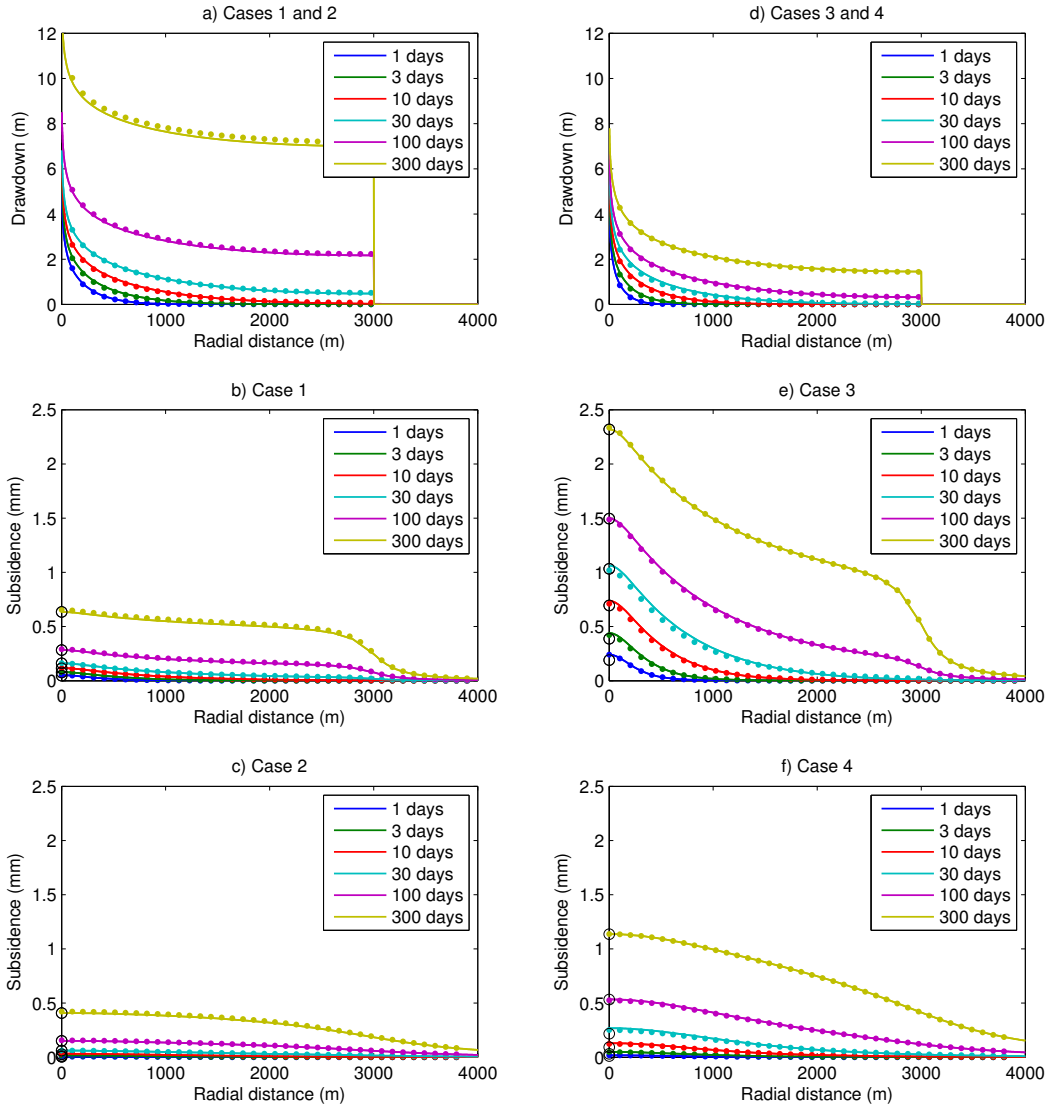

Figure 2: Plots of drawdown (s) and subsidence ($-u_z(r,0)$) for Cases 1 to 4 as indicated by the subtitles. The solid lines were determined using Eq. (12). The circular dots were determined using the finite element simulations. The subsidence values directly above the production well (w), as calculated using Eq. (21), are presented as black circular markers.